

A New Method to Predict Vessel/Platform Dynamics in a Realistic Seaway

S. Vishnubhotla, & J. Falzarano

School of Naval Architecture & Marine Engineering,
University of New Orleans, jfalzara@uno.edu

A. Vakakis

Mechanical Engineering Dept.,
University of Illinois

SUMMARY

In this paper, a recently developed approach (Vishnubhotla, Falzarano and Vakakis, 1998 & 2000) is described which makes use of a closed form analytic solution which is exact up to the first order of randomness, and takes into account exactly the unperturbed (no forcing or damping) global dynamics. The result of this is that, very large amplitude nonlinear vessel motion in a random seaway can be analysed with techniques similar to those used to analyse nonlinear vessel motions in a regular (periodic) seaway. The practical result being that dynamic capsizing studies can be undertaken considering the true randomness of the design seaway. The capsize risk associated with operation in a given sea spectra can be evaluated during the design stage or when an operating area change is being considered. Moreover, this technique can also be used to guide physical model tests or computer simulation studies to focus on critical vessel and environmental conditions, which may result in dangerously large roll motions. In order to demonstrate the practical usefulness of this approach, sample application is included. The results are in the form of solutions, which lie in the stable or unstable manifolds and are then projected onto the phase plane. Finally, the eventual goal of utilizing this method or any other similar method is the development of a physics based ship/platform stability criteria, which can reflect the actual vessel characteristics and operating environment.

1. INTRODUCTION

Research studies of non-linear ship and floating offshore platform rolling motion using dynamical systems' approaches have become quite common (Thompson, 1997). However, practical ship design stability criteria still focus on the static restoring moment curve as the sole or dominant indicator of the vessel's resistance to capsizing and only consider the motion in an implicit or very approximate manner. Most non-linear motions studies are limited to single degree of freedom and regular wave (periodic) excitation with few exceptions (see e.g., Hsieh, et al. (1993), Soliman & Thompson, 1990, and Lin & Yim, 1996). It is well known that roll cannot always be exactly decoupled from the other degrees of freedom but more importantly it is well known that sea waves are not regular but in fact are random. It is common in the design of ships and floating offshore platforms to make narrow banded assumptions and predict short-term extremes using the Rayleigh Probability Density Function (PDF) (see e.g., Ochi, 1998). In this study, the highly non-linear near-capsizing behaviour of a small fishing vessel in a random seaway is analysed by using an analytical solution to the differential equation. The availability of such a closed form solution allows safe basin boundary curves for this pseudo-randomly forced system to be generated.

The *Patti-B* was a small fishing vessel, which has the dubious distinction of having capsized twice. This vessel operated off the United States east coast and was unlucky enough to be involved in two capsizings. Initially she capsized in shallow water and her owners salvaged her

(NTSB, 1979). The second time the vessel capsized in deeper waters and unfortunately all hands were lost.

2. PHYSICAL SYSTEM MODELING

The focus of this study is highly non-linear rolling motion of small fishing vessel possibly leading to capsizing. For the small fishing vessel, the roll axis is the critical motion axis. Roll is in general coupled to the other degrees of freedom; however, under certain circumstances it is possible to approximately decouple roll from the other degrees of freedom and to consider it in isolation. This allows focus on the critical roll dynamics. The de-coupling is most valid for vessels which are approximately fore aft symmetric which eliminates the yaw coupling. Moreover, by choosing an appropriate roll-center coordinate system, the sway is approximately decoupled from the roll (Webster, 1989). For ships, it has been shown in previous studies that even if the yaw and sway coupling are included the results differ only in a quantitative sense. The yaw and sway act as passive coordinates and do not qualitatively affect the roll (Zhang & Falzarano, 1993).

The other issue is the modelling of the fluid forces acting on the hull. Generally speaking, the fluid forces are subdivided into excitations and reactions (Newman, 1982). The wave exciting force is composed of one part due to incident waves and another due to the diffracted waves. These forces are strongly a function of the wavelength / frequency. The reactive forces are composed of hydrostatic (restoring) and hydrodynamic reactions. The hydrostatics are most strongly non-linear and are calculated using a ship hydrostatics computer program. In order that the zeroth order solutions are

expressed in terms of known analytic functions, the restoring moment curve needs to be fit by a cubic polynomial. It should be noted here that it is not much more difficult to utilize a numerically generated zeroth order solution which is based upon an accurate higher order righting arm curve. The hydrodynamic part of the reactive force is that due to the so-called radiated wave force. The radiated wave force is subdivided into added mass (inertia) and radiated wave damping. These two forces are also strongly a function of frequency. However since the damping is light, and for simplicity, constant values at a fixed frequency are assumed. Generally, an empirically determined non-linear viscous damping term is included. However such empirical viscous damping results are only available for ship hulls. The resulting roll equation of motion is :

$$(I_{44} + A_{44}(\omega_n))\ddot{\phi} + B_{44}(\omega_n)\dot{\phi} + B_{44q}\dot{\phi}|\dot{\phi}| + \Delta GZ(\phi, t) = F(t) \quad (1)$$

The focus of this study is non-linear ship rolling motion in a realistic seaway due to a pseudo-random wave excitation. The effect of seaway intensity is accurately considered. In order to obtain the roll moment excitation spectrum, the sea spectrum is multiplied by the roll moment excitation Response Amplitude Operator (RAO) squared (Equation 2a). The RAO for the small fishing vessel in given in Figure 1a.

The sea spectral model used for the small fishing vessel is the Pierson-Moskowitz (P-M). The P-M sea state equation (Ochi, 1998) is as follows,

$$S^+(\omega) = \frac{8.1 \times 10^{-3}}{\omega^5} g^2 e^{-0.074(g/U_w/\omega)^4} \quad (2)$$

Where, U_w is the wind speed. The P-M model is used for this case because it corresponds to a fully developed seaway, which is in some sense the most severe. Moreover, the spectrum is a one-parameter spectrum so that solely the effect of seaway intensity can be considered.

Figures 1b and 1c show the *Patti-B*'s excitation spectra and the corresponding time history of the forcing (in non-dimensional form) for a wind speed of $U_w = 2.75$ meters per second. Figures 2a&b are for larger U_w . The significant wave heights for the sea spectra used for the *Patti-B* range from less than 2.0 foot to almost 7.5 feet. The sea state intensity ranges from about sea state one to four (Bhattacharyya, 1978) which is a reasonable operating condition for the *Patti-B*.

3. THE DYNAMICAL PERTURBATION METHOD

The focus of this investigation is the extension of an approach previously used to study the non-linear dynamics of a small fishing vessel and a very large semi-submersible platform due to pseudo-random wave excitation (Vishnubhotla, Falzarano and Vakakis, 1998

& 2000). The approach is based upon a method originally developed by Vakakis (1993) to calculate in closed form the homoclinic manifolds due to rapidly varying periodic excitation. That approach was generalized to calculate heteroclinic manifolds due to pseudo-random wave excitation. Considering that random excitation is a realistic model for ship and floating offshore platform motions at sea, this method was extended and then applied to consider the case of perturbed heteroclinic manifolds due to an external excitation as approximated by a finite summation of regular (periodic) wave components.

The forcing function would then assume the form shown in equation 3b.

$$S_R^+(\omega) = |RAO|^2 S^+(\omega) \quad (3a)$$

$$F(t) = \sum_{i=1}^N F_M(\omega_i) \cos(\omega_i t + \gamma_i) \quad (3b)$$

where,

$$F_M(\omega_i) = \sqrt{2 S_R^+(\omega_i) \Delta \omega} \quad (3c)$$

The solution to equations such as Equation (1) with softening spring characteristics exhibit two greatly different types of motions depending upon the amplitude of the forcing. For small forcing amplitude, the first type of motion is an oscillatory motion, which is generally bounded and well behaved. For large amplitudes of forcing, the motion can be such that a uni-directional rotation occurs. The boundary between these two types of motions is called in the terminology of non-linear vibrations, the separatrix. This curve literally separates the two qualitatively different motions. In the language of non-linear dynamical systems, these curves are called the (upper and lower) saddle connections. The saddles are connected as long as no damping and forcing are considered in the system. Once damping is added to the system, the saddle connection breaks into stable and unstable manifolds. The stable manifolds are most important, because they form the basin boundary between initial conditions, which remain bounded and those that become unbounded. When periodic forcing is added to the system, these manifolds oscillate periodically with time and return to their initial configuration after one period of the forcing. This forcing period is chosen for the Poincaré sampling time of such a periodic system. Unfortunately, no such obvious Poincaré time sampling exists for the pseudo-randomly forced system studied herein.

In this investigation, the random wave forcing is approximated by a summation of periodic components with random relative phase angles. Although this representation approximates the true random excitation as N64, and)T60, for finite N this does not occur. Actually, the "random" signal repeats itself after $T_R = 2B/T$. Another relevant time period is the average or zero crossing period T_0 . Assuming the spectrum is narrow banded, this might also be a good reference period for a Poincaré map. In lieu of Poincaré maps, we choose to trace out single solution paths, which are

contained in the stable manifolds (see Figure 3). These are then projected onto the phase plane.

The solutions lying in the stable manifolds are calculated using the new approach. This method is a perturbation method, which starts with the un-damped and unforced separatrix. For a simple softening spring (Equation, 4a), this is known in closed form. The critical solutions lying in the stable manifolds are calculated using our approach. This method is a perturbation method that begins with the un-damped and unforced separatrix. For a softening spring, the separatrix is known in closed form. i.e.

$$\ddot{x} + x - kx^3 = 0 \quad (4a)$$

$$x(\tau) = \frac{1}{\sqrt{k}} \tanh\left(\frac{\tau - \tau_0}{\sqrt{2}} + 1/2\right) \quad (4b)$$

$$\dot{x}(\tau) = \frac{1}{\sqrt{2k}} \operatorname{sech}^2\left(\frac{\tau - \tau_0}{\sqrt{2}} + 1/2\right) \quad (4c)$$

The first order solution is determined by using the method of variation of parameters. The original Equation (1), is scaled into the following form,

$$\ddot{x} + x - kx^3 = \varepsilon(-\gamma\dot{x} - \gamma_q\dot{x}|\dot{x}| + F(t)) \quad (5)$$

Having scaled the original equation, the solution method basically involves expanding the solution in a perturbation series as,

$$x(t) = x_0(t) + \varepsilon x_1(t) \dots \quad (6)$$

The second order equation to be solved is actually a linear equation with time varying coefficients. The coefficients are obtained from the zeroth order solution known from Equations (4a) and (5) squared, i.e.,

$$\ddot{x}_1 + x_1 - 3k x_1 x_0^2 = \hat{F}(x_0, t) \quad (7)$$

Solution to the zeroth and first order solution terms yields the perturbed manifolds, which are the boundary between the bounded and unbounded motions. This method explicitly determines the critical solution curves, which separate the bounded steady state oscillatory motions from the unbounded motions. These solutions are determined by solving equations (4) and (5) and using them in (6).

The approach taken in this paper although different from our previous analysis is similar enough that all the details need not be completely repeated herein. The basin boundaries correspond to the stable manifolds associated with the positive and negative angles of vanishing stability and are just the damped and forced extensions to the upper and lower separatrices respectively which were previously discussed. These stable manifolds form the basin boundary between bounded (safe, non-capsizing) and unbounded (capsizing) solutions. See for example Figure 3a.

Although this method was originally developed by Vakakis (1993) to study intersections of stable and unstable manifolds for equations for which the Melnikov method could not be used, this method is applied herein because it is general enough to yield exact solutions to general equations such as the multiple frequency forcing case being studied herein.

4. RESULTS

The results are for the roll of a small fishing vessel which is probably one of the smallest vessels to venture away far from safety of shore. For the range of seaway considered, the results exhibit qualitatively different types of behaviour; even for these mild seaways considered herein.

An indication of if the basin boundaries will be simple and smooth or fractal and complicated is determined by if the manifolds intersect or not. As a first step in determining whether or not this will occur for the pseudo-randomly forced system is to determine solutions, which lie in both the stable and unstable manifolds. After this is done, the distance between the two solutions can then be determined and this will indicate whether or not a manifold intersection has occurred. When the distance between the two manifolds goes to zero, the manifolds become tangent and this is a critical value of the forcing. Beyond the value of forcing where the manifolds become tangent the manifolds intersect and the safe basin begins to erode. This is exactly what the Melnikov function (Falzarano, et al, 1992) is used for and what is being described herein is simply a more general alternative to the Melnikov approach. The method described herein has several potential benefits over the classical Melnikov approach. These benefits enable the ability to, 1) analyse very general systems for which the Melnikov method is not valid 2) obtain higher order results, and 3) develop a visual projection of the manifolds for single degree of freedom systems.

4.1 Safe Basin Boundary Projected Phase Plane

The results are for physical parameters representing the clam dredge *Patti-B* (Falzarano, et al., 1992) in beam seas and rolling in various intensity Pierson-Moskowitz sea spectra. As stated previously, the sea spectra are approximated by a finite but large number of periodic components. As can be seen, when the wind speed is increased and the seaway intensity increases, the vessel's dynamics change qualitatively. The upper and lower stable manifolds change from smooth curves similar to the unforced system to rather complicated curves indicating the possibility of manifold intersections. The size of the safe operating region of the vessel is somewhat related to when these manifolds intersect and become fractal or complicated. Figures 2a, b & c show moderate to large amplitude sea spectra plotted versus frequency for a range of wind speeds. The wind speed is the single parameter describing the seaway intensity.

Results for time-varying roll motion solutions contained within the upper and lower stable manifolds projected phase planes for these sea spectra are given in Figures 3a-3c. One can see that Figures 3a&b show smooth stable manifolds while Figure 3c shows tangled stable manifolds. When looking at these projected phase plane results, it should be recognized that the solutions depicted represent a time evolution of a single trajectory and are not Poincaré time samplings of the manifold. This explains the wrapping around the fixed point. The random oscillation occurs on the average at the zero crossing period while the solution is slowly evolving towards the fixed point.

4.2 Extended State Space Results

However, once unstable manifolds are also included, the two-dimensional projection of the time-varying solutions, lying in the stable or unstable manifolds, may look deceptive. This is so because true intersections only occur for the same time phase. Therefore a three-dimensional extended state space representation is the only unique representation. In order to illustrate this and in order to determine whether or not intersections have occurred, some typical results for the *Patti-B* are provided. These one-dimensional solution curves are shown in the full three-dimensional extended state space (Fig. 4). These results clearly indicate that the two curves do not intersect for the two given seaway intensities.

A more extensive and systematic investigation is currently underway. In order to more clearly determine if the manifolds intersections have occurred the entire manifold must be generated. Generating the entire manifold would involve varying the initial time t_0 and then generating an entire manifold mesh. After this had been done, the distance between the two manifolds, i.e., stable and unstable can then be calculated. This distance going to zero would indicate that manifold intersections were imminent. This would be a critical value of external wave forcing since at a greater value of wave forcing, the safe basin would begin to erode.

5. CONCLUSIONS

The method utilized herein is quite powerful and capable of handling very general systems. The application herein utilized the knowledge of the zeroth order solution, which was known in closed form for this simple system. However, this is not a requirement and actually for more general systems it could be known numerically. Clearly, the safe operating region of the vessel is directly related to when the calculated stable and unstable manifolds intersect and erode the safe basin. It should be re-emphasized here that the results given correspond to single realizations of the given sea spectra. In order to gain a more complete probabilistic understanding of the systems random behaviour, multiple realizations must be considered and analysed. This ensemble of results should then be analysed in terms of averages and standard

deviations. However, this has not yet been done in a systematic manner.

The results clearly demonstrate the effect of random excitation on the global dynamics of the vessel about its roll axis. Finally, the eventual goal of utilizing this method or any other similar method is the development of a physics based ship/platform stability criteria, which reflects the actual vessel characteristics and operating environment. Moreover, such a physics based method can be used to gain insight into the importance of relevant capsizing mechanisms in addition to what has been studied herein. Obviously, much more work needs to be done before such a stability criteria is a reality. Some of this work has begun but much more remains to be done.

6. ACKNOWLEDGMENTS

The authors would like to acknowledge the support of the US National Science Foundation, Dynamical Systems and Control Program and program manager Dr. Alison Flatau.

7. REFERENCES

- Bhattacharayya, R., *Dynamics of Marine Vehicles*, Wiley, New York, 1978
- Falzarano, J., Shaw, S., & Troesch, A., "Application of Global Methods for Analysing Dynamical Systems to Ship Rolling Motion and Capsizing," *International Journal of Bifurcation and Chaos*, Vol. 2, #1, (1992).
- Hsieh, H., Shaw, S. & Troesch, A., "A Predictive Method for Vessel Capsize in a Random Seaway," *Nonlinear Dynamics of Marine Vehicles*, ASME (1993)(Ed. J. Falzarano & F. Papoulas).
- Lin, H and Yim, S., "Chaotic Roll Motion and Capsizing of Ships Under Periodic Excitation with Random Noise," *Applied Ocean Research*, Vol. 117, 1995.
- National Transportation Safety Board (NTSB), "Grounding and Capsizing of the Clam Dredge *Patti-B*," *NTSB Marine Accident Report*, 1979.
- Newman, J, *Marine Hydrodynamics*, MIT Press, Cambridge (USA), 1982.
- Ochi, M, *Ocean Waves*, Cambridge University Press, Cambridge (UK), 1998.
- Soliman, M. & Thompson, JMT, "Stochastic Penetration of Smooth and Fractal Basin Boundaries under Noise Excitation," *Dynamics and Stability of Systems*, Vol. 5, (1990)
- Thompson JMT, "Designing Against Capsize in Beams Seas: Recent Advances and New Insight," *Applied Mechanics Reviews*, Vol. 50, No. 5, May 1997.

Vakakis, A., (1993), "Splitting of Separatrices of the Rapidly Forced Duffing Equation," *Nonlinear Vibrations*, ASME Vibrations Conference, September.

Vishnubhotla, S., Falzarano, J. and Vakakis, A., (1998), "A New Method to Predict Vessel/Platform Capsizing in a Random Seaway," *3rd International Conference on Computational Stochastic Mechanics*, Balkema, Holland.

Vishnubhotla, S., Falzarano, J. and Vakakis, A., (1998), "A New Method to Predict Vessel/Platform Capsizing in a Random Seaway," *Philosophical Transactions of the Royal Society*, Special Issue on Nonlinear Dynamics of Ships, May 2000.

Webster, W., "The Transverse motions," Chapter 8 Seakeeping, *Principles of Naval Architecture Volume III*, Society of Naval Architects and Marine Engineers, New York, 1989.

Zhang, F. and Falzarano, J., "Multiple Degree of Freedom Global Transient Ship Rolling Motion: Large Amplitude Forcing," *Stochastic Dynamics & Reliability of Nonlinear Ocean Systems*, ASME (1994).

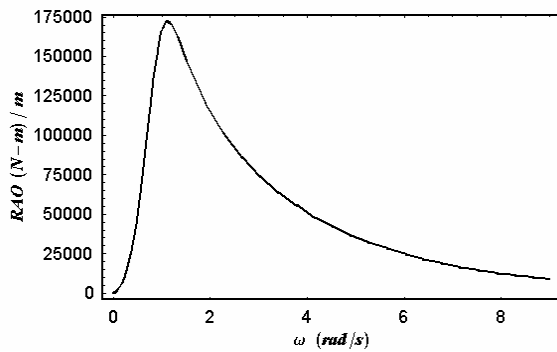


Fig 1a. *Patti-B* Roll Moment Excitation Transfer Function (RAO)

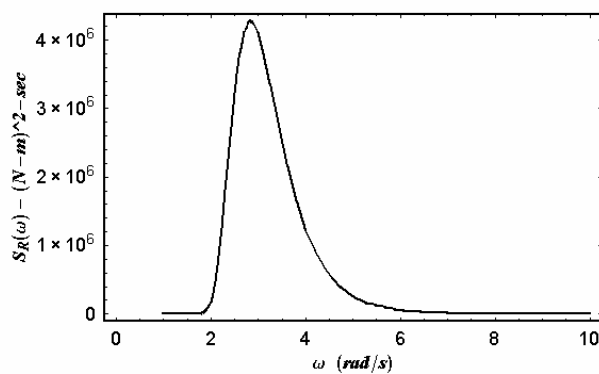


Fig 1b. *Patti-B* Roll Moment Excitation Spectrum, $U_W = 2.75 \text{ ms}^{-1}$

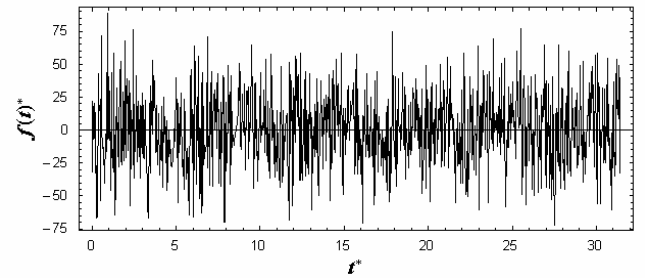


Fig 1c. *Patti-B* Corresponding Roll Moment Excitation Time History (non-dim), $U_W = 2.75 \text{ ms}^{-1}$

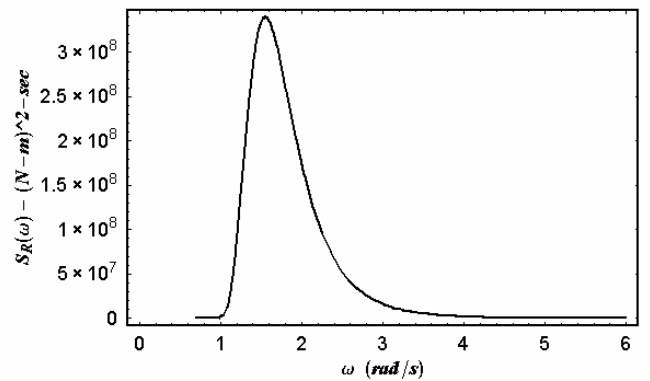


Fig 2a. *Patti-B* Moderate Amplitude Roll Moment Excitation Spectra, $U_W = 5.15 \text{ ms}^{-1}$

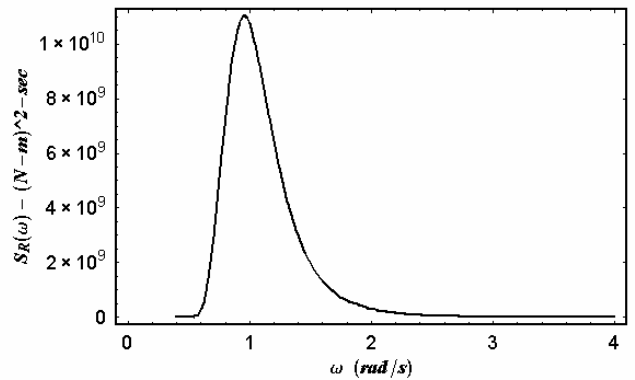


Fig 2b. *Patti-B* Large Amplitude Roll Moment Excitation Spectra, $U_W = 10.0 \text{ ms}^{-1}$

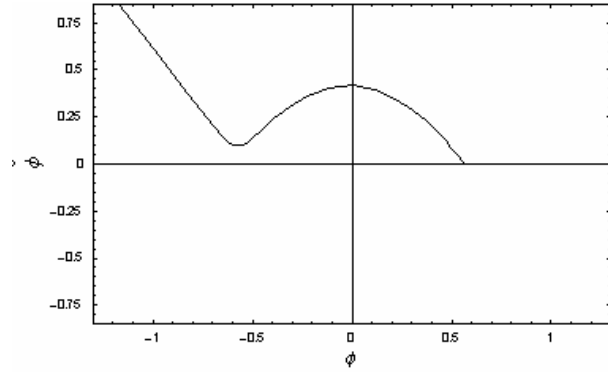


Fig 3a. *Patti-B* Projected Phase Plane for P-M Spectra,
 $U_W = 2.75 \text{ ms}^{-1}$

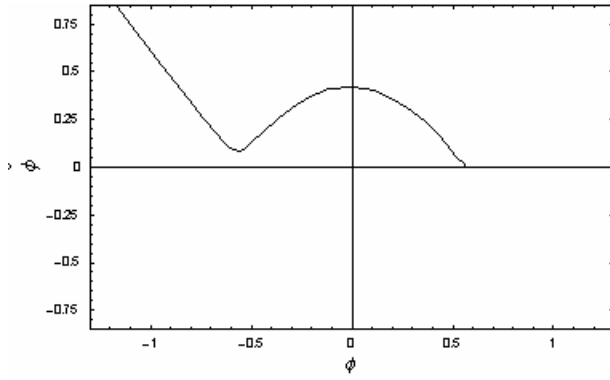


Fig 3b. *Patti-B* Projected Phase Plane for P-M Spectra,
 $U_W = 5.15 \text{ ms}^{-1}$

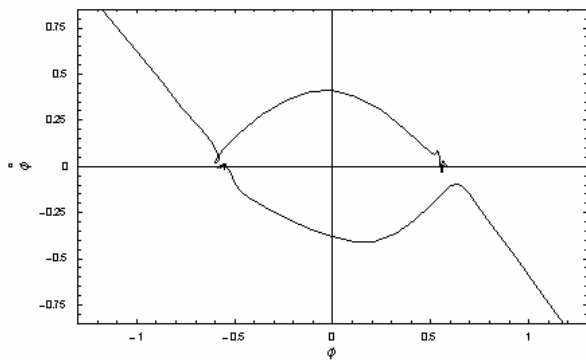


Fig 3c. *Patti-B* Projected Phase Plane for P-M Spectra,
 $U_W = 10.0 \text{ ms}^{-1}$

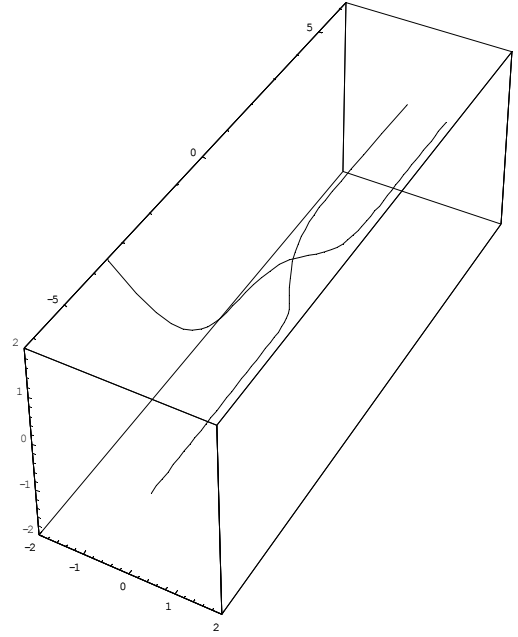


Fig 4a. *Patti-B* Extended Phase Space showing solutions
contained in upper stable, $W^{+s}(t)$ and lower unstable
manifold $W^{-s}(t)$, $U_W = 2.75 \text{ ms}^{-1}$

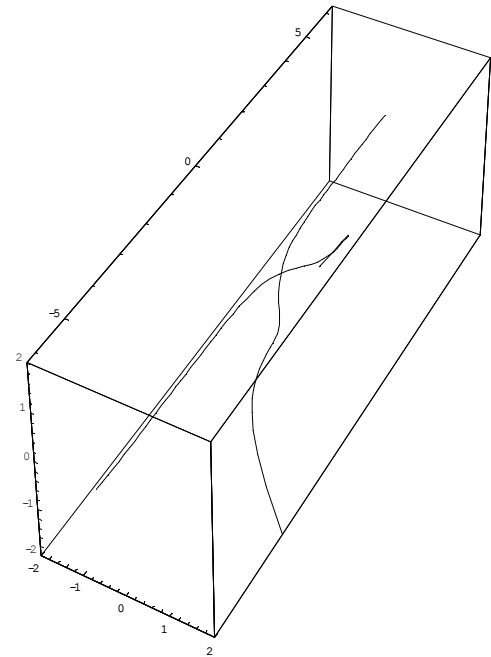


Fig 4b. *Patti-B* Extended Phase Space showing solutions
contained in upper unstable, $W^{+us}(t)$ and lower stable
manifold $W^{-s}(t)$, $U_W = 2.75 \text{ ms}^{-1}$